Corrosion of unglazed rough graphite-aluminium solar absorber surfaces in simulated acid and neutral rain

P. Konttinen[*a]**, T. Salo**[b]**, P.D. Lund**[a]

[a]Advanced Energy Systems Laboratory, P.O. Box 2200, Helsinki University of Technology, FIN-02015 HUT, Finland
[b]Laboratory of Corrosion and Material Chemistry, P.O. Box 6200, Helsinki University of Technology, FIN-02015 HUT, Finland

Abstract

Degradation mechanisms of unglazed solar absorber surfaces based on aluminium substrate were studied. Rough graphite-aluminium surfaces were total-immersion subjected to aerated and de-aerated simulated neutral and acid rain. Test conditions were based on calculated absorber stagnation temperature and global rain acidity measurements. Changes in optical properties, elemental composition and sample mass were examined by spectrometry, energy dispersive X-ray spectrometry and thermogravimetry, respectively. The absorbers exhibited almost no degradation at pH value of 3.5. At pH 5.5 alumina on the surface hydrated significantly degrading the optical properties of the surfaces severely in most cases. Therefore these absorber surfaces can not be recommended to be used in nonglazed applications if they are exposed to rain with pH exceeding ~3.5 – 4.5. The total-immersion test needs to be developed further as the test results exhibited poor temperature and time dependency thus preventing accurate service lifetime estimates. Still, these tests were useful in determining favourable and non-favourable operating conditions for the absorber surfaces based on aluminium substrate.

Keywords: accelerated aging, acid rain, unglazed solar absorber, aluminium substrate

1. Introduction

Unglazed solar absorbers are subject to some of the ambient conditions such as rain, wind and deposits more severe than absorber surfaces inside covered collectors. Again, temperature of uncovered collector remains lower in stagnation conditions causing less temperature induced stress on the surface. Complexity of the possible degradation mechanisms and their interactions make it difficult to estimate the effect of different ambient factors on the lifetime of an unglazed absorber. Long term measurements of degradation of unglazed absorbers would be needed in order to verify laboratory test results. Corrosive effect of deposits remaining on the surfaces due to rain, dust, ice, etc. should be studied as well. However, the effect of individual factors can be examined in laboratory conditions in order to provide a picture of their influence on the behaviour of the absorber in the corrosive medium. This will aid in deciding whether the operating conditions are favourable or unfavourable to the corrosion resistance of the absorber.

---

[*] Corresponding author. Tel.: +358-9-4513212; fax: +358-9-4513195; E-mail: petri.konttinen@hut.fi, member of ISES

Widely accepted methods (draft proposal ISO/CD 12592,2) have been developed for testing the service lifetime of solar absorber surfaces inside glazed collectors (Brunold et al., 2000a, Brunold et al., 2000b, Carlsson et al., 1994, Carlsson et al., 2000a, Carlsson et al., 2000b). Tests are conducted under three different conditions: 1) high temperatures and low humidity, 2) service temperatures under condensation conditions and 3) service temperatures and high humidity air containing SO_2. However, the set-up cost estimate of SO_2 –testing equipment is over 50,000 € (Möller, 2000). Modifying the SO_2 –test chamber or a standard climate chamber for acid rain operation could add to the costs significantly. Instead, we used relatively low-cost total-immersion equipment based mainly to the recommendations in (Shreir et al., 1994). All the samples were of selective rough graphite-aluminium absorbers (Konttinen et al., 2003a, Konttinen et al., 2003b). These absorbers consist of a carbon (probably mainly in graphite form, see (Konttinen et al., 2003a) for details) and alumina containing heterogeneous matrix structure on an aluminium substrate sheet. The samples used comply with the optical homogeneity standard deviation limits defined for the glazed collector solar absorber surface tests (Brunold et al., 2000b). Changes in optical properties were determined by UV-Vis.-IR spectroscopy. Some of the samples were analysed by thermogravimetry (TG) and energy dispersive x-ray spectroscopy (EDS). pH levels chosen for the tests were based on the global acid rain measurements (Howells, 1990). Metal corrosion studies in simulated acid rain (Magaino, 1997, Magaino, 1999) and corrosion studies of carbon fiber (graphite) – aluminium metal-matrix composites (Hihara, 1997, Hihara and Latanision, 1994) were used as first guidelines for designing the tests and analysing the corrosion behaviour of graphite-aluminium solar surfaces in simulated acid rain. In condensation tests according to draft proposal ISO/CD 12592,2 the main degradation mechanism of graphite-aluminium solar surfaces has been found to be hydration of aluminium oxide (Konttinen and Lund, 2003).

2. Experimental

For determining the appropriate temperature levels for the tests stagnation temperature for an unglazed absorber was calculated iteratively (Eq. 1) for each hour of the year based on the energy balance equations in (Duffie and Beckman, 1991):

$$T_s = \frac{\alpha \cdot G_T - \left(\varepsilon \cdot \sigma\left(T_s^4 - T_{sky}^4\right)\right)}{2.8 + 3 \cdot V} + T_a , \tag{1}$$

where T_s is the stagnation temperature, α is the solar absorptance (AM 1.5), G_T is the global irradiance, ε is the thermal emittance of the absorber (at 100°C), σ is the Stefan-Boltzman constant, T_{sky} is the sky temperature ($T_{sky} = T_a - 6$), T_a is the ambient temperature and V is the wind speed. Hourly weather data (G_T, T_a and V) of a reference year (Helsinki, 1979) was used for calculations. Collector area of 12 m^2 and slope $\beta = 0$ were fixed. The results for an absorber having $\alpha = 0.90$ and $\varepsilon = 0.22$ (best optical properties obtained so far for the rough graphite-aluminium surface) are shown in Fig. 1. Real absorber temperature is typically less than the stagnation temperature as heat is extracted under the surface.
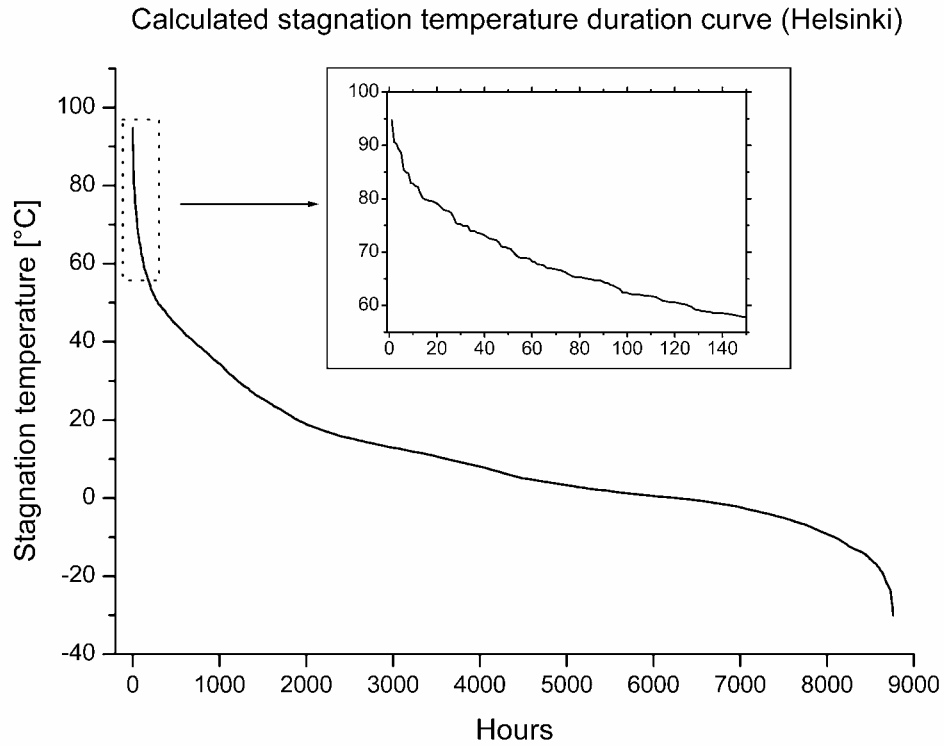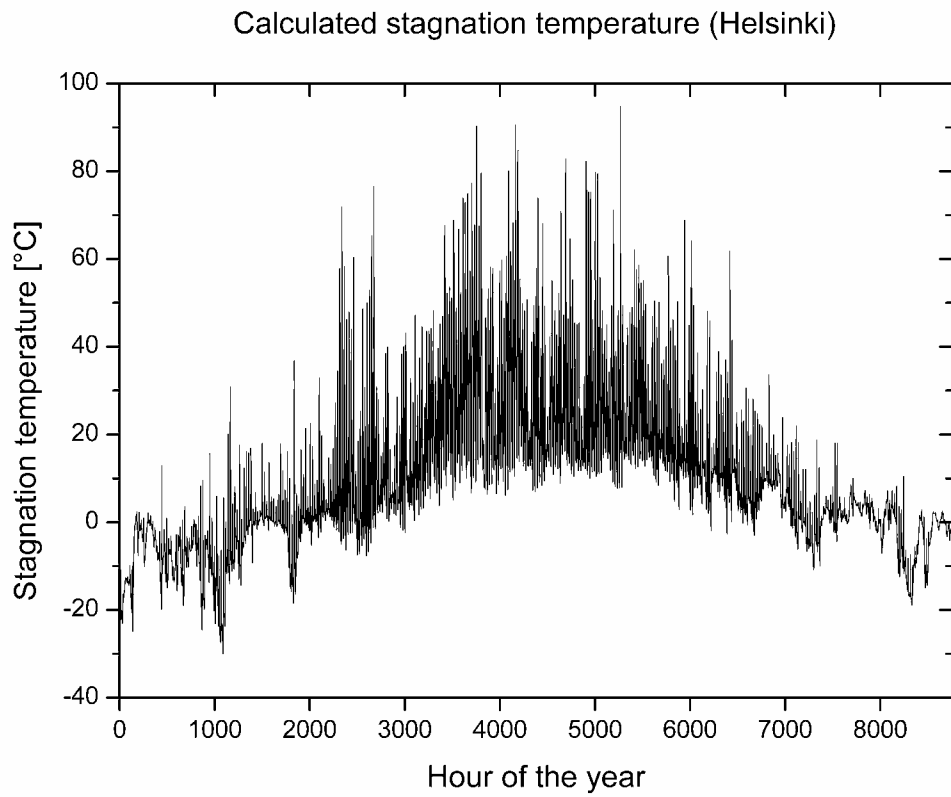
Figure 1. Calculated stagnation temperatures and duration curve in Helsinki for a rough $C/Al_2O_3/Al$ absorber having $\alpha = 0.9$, $\varepsilon = 0.22$.

Surface samples were immersion subjected (Fig. 2) to O_2-aerated or zero-aerated (with N_2) simulated acid rain (Table 1) with pH = 3.5 or 4.5 and simulated neutral rain with pH = 5.5 in temperatures of 60, 80 or 99 °C. Saturating gas was fed at room temperature into the solution. The flask was heated within ±1 K of the required temperature in a paraffine oil bath, which was typically 6-10°C (at 60/80°C) or 40-45°C (at 99°C) warmer than the solution inside the flask.
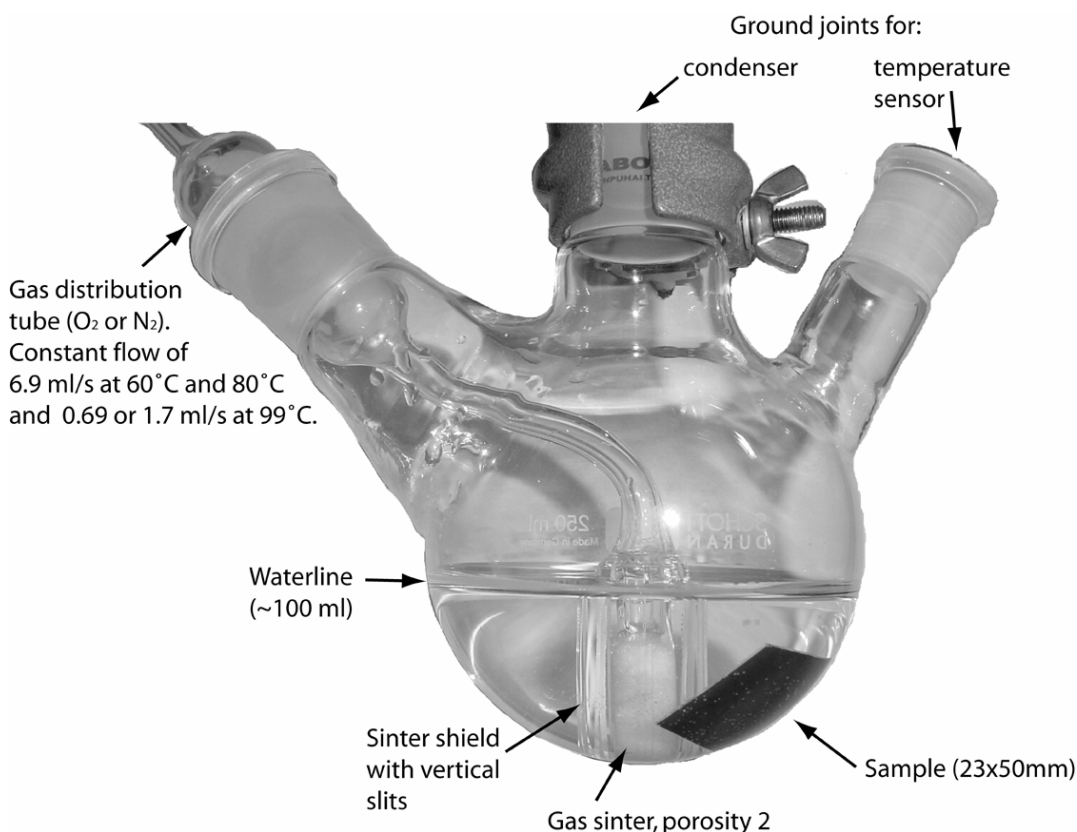

Figure 2. Photograph of the acid rain total-immersion setup including 250 ml three-necked flask, 100 ml simulated acid rain, 23 x 50 mm sample and gas distribution tube (excluding heating system consisting of paraffine oil bath, heater and temperature controller).

Samples tagged as ''non-aerated'' in tables and figures were tested with impedance spectroscopy at similar temperatures and pH. These results will be published separately. Changes in optical properties and elemental composition of non-aerated samples are included in this paper for comparison to aerated and zero-aerated test results.

Hemispherical reflectance of the samples was measured before and after each test at room temperature. Solar absorptance, α, was determined between 0.39 – 1.1 µm with a LI-COR LI-1800 type spectroradiometer and a $BaSO_4$ coated integrating sphere. Thermal emittance, ε, was determined between 2.5 – 20 µm with a MIDAC Prospect FTIR-spectrometer with a semi-hemispherical integrating device. Spectral reflectance, ρ_λ, was analysed for estimating the hydration levels of alumina.

Table 1. Chemical composition of the simulated acid rain. pH = 3.5 adapted from [12]. pH values of 4.5 and 5.5 gained by adjusting the amount of NO_3^- and SO_4^{2-}.

Ion	Concentration/mg dm^{-3}		
	pH = 3.5	pH = 4.5	pH = 5.5
F^-	0.098	0.098	0.098
Cl^-	1.0	1.0	1.0
NO_3^-	7.1	0	0
SO_4^{2-}	9.8	1.5	0.15
Na^+	0.42	0.42	0.42
K^+	0.11	0.11	0.11
Ca^{2+}	0.049	0.049	0.049
Mg^{2+}	0.051	0.051	0.051

Thermogravimetry (Mettler TA thermal analysis system) was applied for determining the mass changes of some of the samples exposed to acid rain tests. The Mettler system consists of a TC11 TA processor, a TG50 thermobalance and a M3 microbalance. The samples were heated up from 30°C to 500°C at a constant rate of 10°C/min and cooled down to 30°C at an equal rate.

Test duration needed to degrade the α and ϵ according to performance criteria (PC) was determined in each test:

$$PC = -\Delta\alpha + 0.25\Delta\epsilon \leq 0.05 \qquad (2)$$

Eq. 2 is typically used failure limit for solar absorbers inside glazed collectors (Brunold et al., 2000a, Brunold et al., 2000b, Carlsson et al., 1994, Carlsson et al., 2000a, Carlsson et al., 2000b, Hollands et al., 1990, Lampert, 1989). PC value of 0.05 is generally equivalent to 5 percentage unit decrease of the solar heat gain by the flat-plate solar collector water heating system. Although not defined for unglazed collectors, Eq. 1 was taken as a failure limit for easy comparison to commonly used (glazed) solar absorber accelerated aging test results. In addition, we used Eq. 1 as there is no similar widely used performance criteria defined for unglazed collector surfaces.

3. Results

3.1. Changes in solar absorptance and thermal emittance

Absorptance changes were generally larger and occurred faster at lower pH values (Fig. 3). Changes in emittance were mainly the opposite, i.e. larger at lower pH values (Fig 4). The resulting PC values (Eq. 2.) were almost in all cases within the acceptable limit at pH 3.5, distributed both side of the limit at pH 4.5, and generally above the acceptable limit at pH 5.5 (Fig. 5).
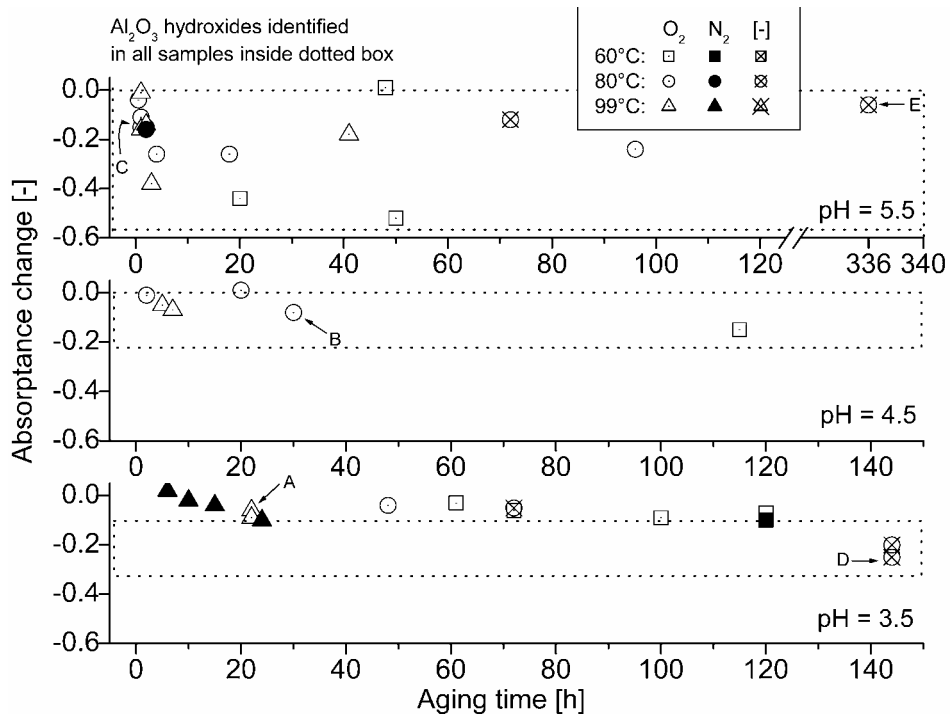
Figure 3. Changes in solar absorptance for samples exposed to simulated acid rain immersion tests. Samples analyzed with EDS denoted as A-E.
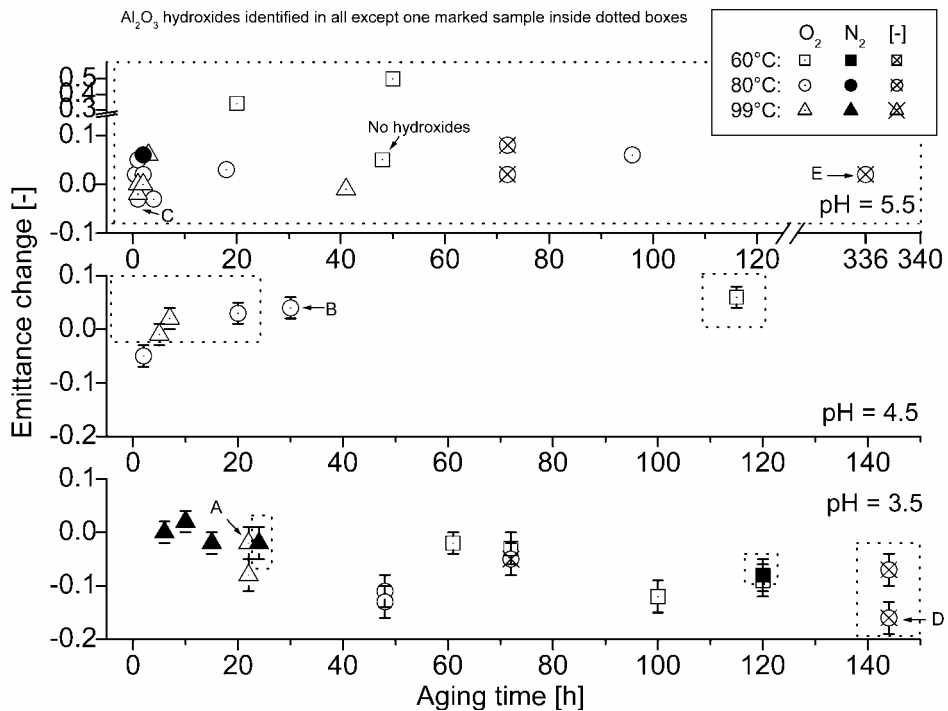

Figure 4. Changes in thermal emittance for samples exposed to simulated acid rain immersion tests. Error limits shown when larger than symbol size. Samples analyzed with EDS denoted as A-E.
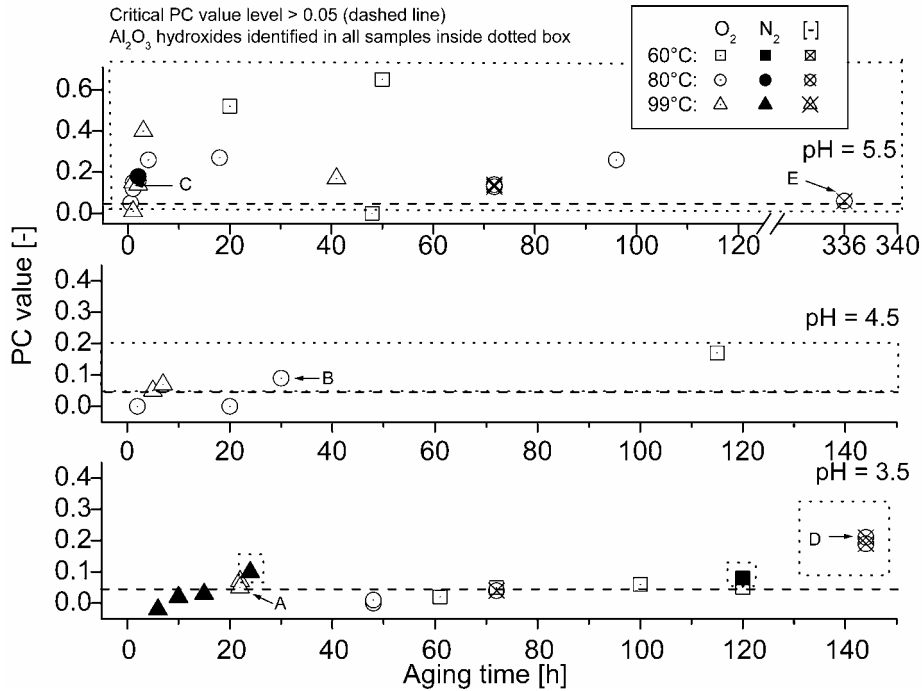
Figure 5. PC values for samples exposed to simulated acid rain immersion tests. Samples analyzed with EDS denoted as A-E.

The majority of the samples exhibited neither specific temperature-depending nor gasification type/rate – depending behaviour. In addition, there is no clear difference in degradation between the O_2, N_2 or non-aeration or the rate of aeration at any pH level. It seems that the pH level is the major determinant regarding to the degradation rate. Unfortunately, there was large deviation especially in the absorptance results at pH 5.5 exposure times between 0.5h and 4h.

In previous condensation tests for similar samples with de-ionized water according to draft proposal ISO/CD 12592,2 (Brunold et al., 2000a) all the samples exhibited Arrhenius-type temperature and time dependent degradation (Konttinen and Lund, 2003). Complexity of the simulated acid rain test method including multiple variables makes it difficult to determine the reasons for non-Arrhenius type behaviour. The most likely reason is uncontrolled movement of the acid rain solution causing irregular chemical reactions. Futhermore, the primary assumption of the combined effect of gas feeding and natural convection being sufficient for moving the solution seems to be inadequate. The amount of reactants in the solution is quite small (Table 1). Therefore small variations in solution composition can have caused different results as well.

3.2 Energy dispersive x-ray spectrometry

Energy dispersive x-ray spectrometry (EDS) was used for determining the changes in elemental composition due to acid rain exposure. The equipment consists of a Scanning Electron Microscope LEO 1450 and INCA Energy 300 Microanalysis System (EDS).

Samples analysed by EDS are presented in Table 2 and in Figs. 3-5 denoted as A-E. For enhancing the analysis accuracy, other samples but REF2 were double carbon

coated after the acid rain exposure but prior to the EDS analyses. The elemental composition of the analysed surfaces is presented in Table 3. Unaged sample REF 2 consists of approximately 4 % of C, 47 % of O, 48 % of Al and less than 1 % of Si, which is in accordance with the earlier EDS analyses (Konttinen et al., 2003b). Carbon was omitted from the analyses for the other samples due the to additional carbon coating. All of the aged samples show clear increment in O and decrease in Al, thus indicating oxidation of aluminium and/or hydration of alumina (hydrogen is not detectable with EDS).

Most of the aged samples contain < 1% of F, Na, S and/or Cl. It is hard to draw any conclusions on the corrosion effect of such a small quantities, as the variation in $\Delta\alpha$ and $\Delta\varepsilon$ are relatively large between the samples. Only samples A and D exposed to pH 3.5 contain more of S (4% and 5%, respectively). However, α and ε of the aerated sample A changed significantly less than α and ε of non-aerated sample D, and therefore the increased amount of S alone can not explain the variety in optical changes. It may be possible that the increased amount of Cl is responsible for the additional corrosion for sample D.

Table 2. Samples analysed by SEM and EDS. Coating method prior to analyses shown in remarks.

Sample	Sample remarks, coating method prior to analyses	pH	T [°C]	t [h]	$\Delta\alpha$	$\Delta\varepsilon$	PC	Aeration rate
A	Double carbon coating	3.5	99	22	-0.06	-0.02	0.05	O_2 6 l/h
B	Double carbon coating	4.5	80	30	-0.08	0.04	0.09	O_2 25 l/h
C	Double carbon coating	5.5	80	1	-0.15	-0.03	0.15	O_2 25 l/h
D	Double carbon coating	3.5	80	144	-0.25	-0.16	0.21	No aeration
E	Double carbon coating	5.5	80	336	-0.06	0.02	0.06	No aeration
REF 1	Unaged reference sample, double carbon coating	-	-	-	-	-	-	-
REF 2	Unaged reference sample, no carbon coating	-	-	-	-	-	-	-

Table 3. Elemental composition in percentage of the surface of the samples analysed by EDS. Carbon omitted due to additional carbon coating prior to the analyses from all other but uncoated sample REF 2.

Sample	C	O	F	Na	Al	Si	S	Cl
A	-	56	< 1	< 1	38	< 1	4	-
B	-	59	1	< 1	38	< 1	< 1	-
C	-	60	1		38	< 1	-	-
D	-	54	-	-	34	< 1	5	3
E	-	59	1	< 1	37	2	< 1	< 1
REF 1	-	47	-	-	53	< 1	-	-
REF 2	4	47	-	-	48	< 1	-	-

3.3. FTIR spectroscopy analyses of the hydration level of the Al_2O_3/Al substrate

FTIR-spectrometry has been used for analysing the hydroxide films on aluminium by Takahashi et al (Carlsson et al., 1994, Takahashi et al., 1987). Based on the characteristic absorption bands (for details, see (Takahashi et al., 1987)) related to the different hydroxides Tanemura et al (Carlsson et al., 1994, Tanemura et al., 1990) have analysed the hydration level of Ni pigmented anodized aluminium absorber surfaces. Similar to these, the main degradation mechanism of graphite-aluminium solar absorber surfaces have been found to be hydration of aluminium oxide (mainly) to pseudoboehmite and boehmite (Konttinen and Lund, 2003). It is possible that during the hydration process the thin carbon layer (Konttinen et al., 2003a) on the surface is oxidated through chemical reactions forming CO, CO_2 and other compounds (Hihara and Latanision, 1994). The revealed Al_2O_3 layer subsequently probably follows typical alumina-aluminium corrosion mechanisms. We used FTIR-spectroscopy for determining the hydration level of the absorber substrate, consisting of thicker than naturally formed heterogeneous alumina layer on 0.5 mm thick aluminium substrate of 99.5 % purity.

The combined results are shown in Figs. 3-5. All samples inside dotted boxes contain identified Al_2O_3 hydroxides i.e. pseudoboehmite and/or boehmite, possible other forms of hydroxides as well (e.g. bayerite and gibbsite). Detailed analyses of the results show that hydroxides are identified in all but one sample exposed to pH 5.5. The most degraded samples (PC > 0.18) have absorption bands related to both pseudoboehmite and boehmite (Fig. 6), whereas the rest of the hydrated samples do not have the characteristic absorption band of pseudoboehmite.

3.4 Thermogravimetry analyses

According to (Tanemura et al., 1990) pseudoboehmite is transformed to boehmite after heating due to the outgassing of excess water and then being transformed to aluminium oxide without any water inside of the structure at the temperature higher than 300°C. We used thermogravimetry (TG) analyses to determine the possible mass changes and the related water outgassing in a few of the samples. The results show (Fig. 6) that only the most degraded samples (PC ≥ 0.5) exhibit clearly measurable mass changes between 230°C and 280°C. For samples degraded to PC ≤ 0.21 no temperature specific changes were detected within the measurement accuracy. The combined mass of carbon reacted to CO_2 and outgassed water may be too small to be measured for these samples with the TG equipment used.
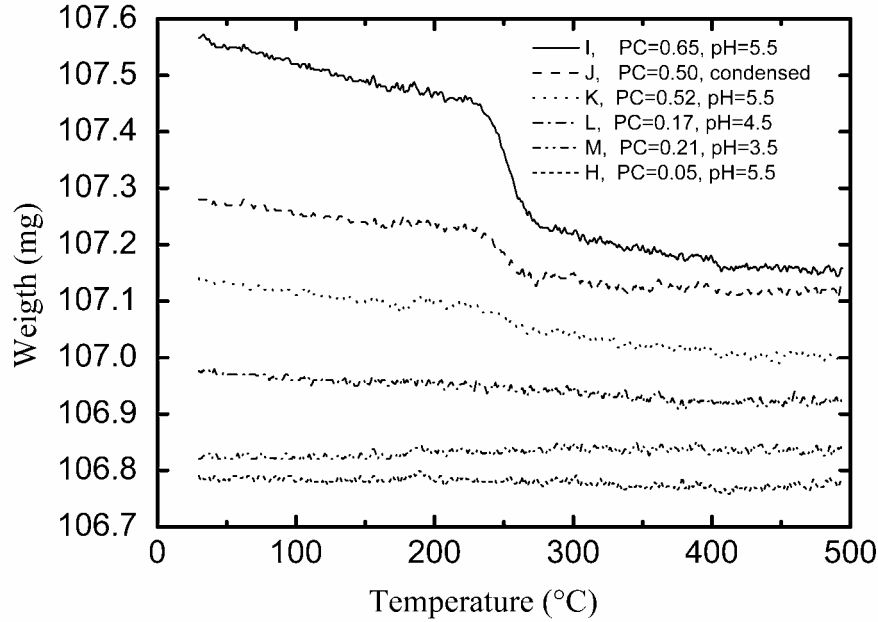
Figure 6. Thermogravimetry (TG) curves for most degraded samples at each pH between 30°C and 500°C at a heating rate of 10°C/min. A reference sample G was exposed to condensed ion-exchanged water inside a climate chamber. All TG-analysed samples having PC ≈ 0.05 exhibit behaviour similar to sample K regardless of the pH. Curves shifted max. 0.5 mg up or down for clarity.

4. Discussion

The amount of water in the air during rain can be determined with Eq. 2 (Tarvainen, 2003):

$$L = \left(\frac{200 \cdot R^{1.6}}{24000} \right)^{\frac{1}{1.82}} , \tag{2}$$

where L is the amount of water in air (g m^{-3}) and R is the intensity of rain (mm h^{-1}). However, for simulating heavy rain (10 mm h^{-1}) inside a water flask containing 100 ml of simulated rain water, almost 200 m^3 of air would be needed per hour.

Total-immersion test results were compared to standard condensation test results (Konttinen and Lund, 2003) in order to determine correlation between the two methods. Samples degraded to PC=0.05 in total-immersion tests exhibit generally similar ρ_λ as the samples degraded to PC=0.05 in standard condensation tests (Fig. 7, cf. Fig. 3 in (Konttinen and Lund, 2003)). Fig. 8. shows the ρ_λ of the most degraded sample (PC = 0.65) and a sample subjected to condensation in a climate chamber about equal time at the same temperature (PC = 0.50). The difference between these two is the higher α (but similar form of α_λ) of the former and lack of (or smaller) absorption bands between 4 and 6 μm and 6.5 – 8.5 μm. Otherwise the spectral reflectances are quite similar.
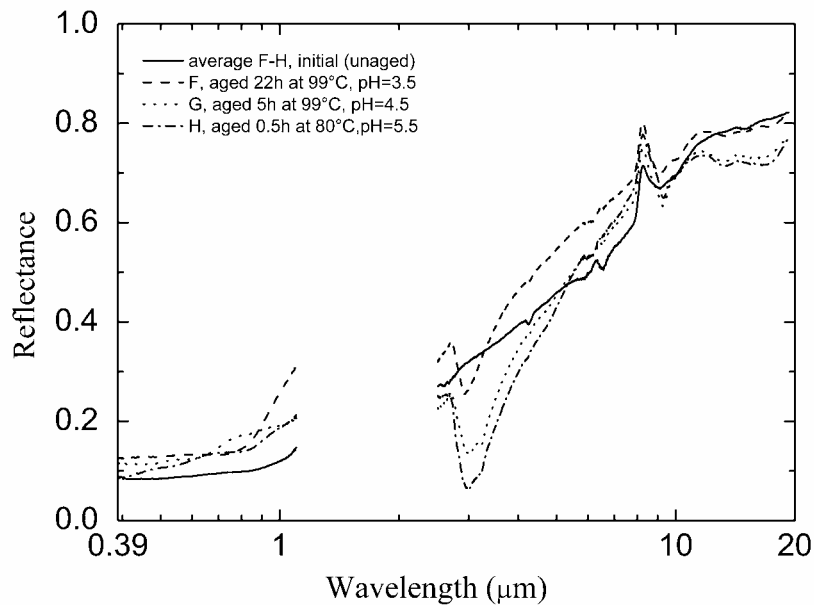
Figure 7. Spectral reflectance of the samples degraded to PC = 0.05 level at each pH.
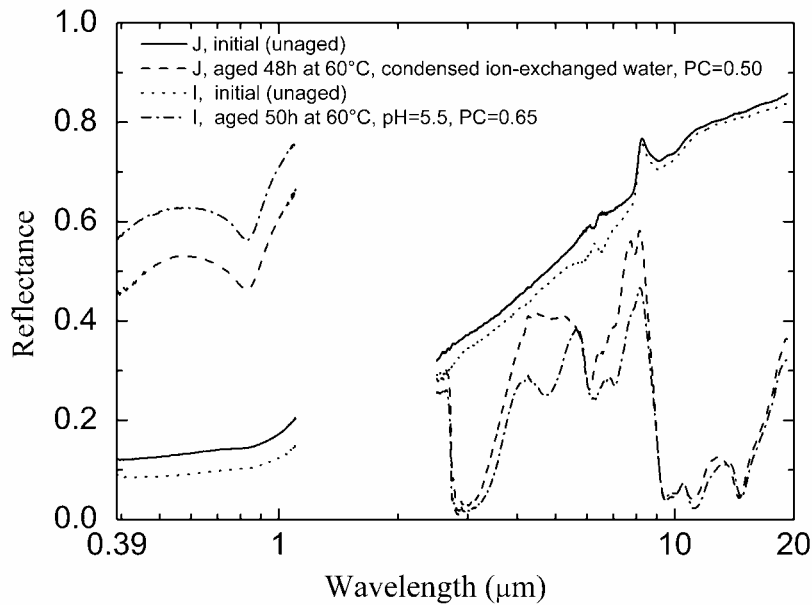

Figure 8. Spectral reflectance of the most degraded sample and a reference sample subjected to an ion-exchanged water condensation test.

Still, when comparing all the optical results (Figs. 3-5) we can conclude that total-immersion method without controlled solution movement turned out not being optimal as the samples did not exhibit clearly detectable temperature and time dependencies.

This method was chosen instead of e.g. rotating disk method (Magaino, 1997) because impedance spectroscopy tests required the use of a liquid electrolyte in contact with the sample. We assumed that the gas feed and natural convection would rotate the solution inside the flask sufficiently enough for reproducible test results. It seems that this was not the case at least at pH = 5.5. A controlled solution or sample movement (combined with controlled temperature and gas feeding rate) should be implemented in the future tests.

Semi-integrating device attached to the FTIR-spectrometer increases interference thus disturbing the exact determination of precise absorption peaks. Therefore we had to make rougher analyses of absorption bands.

Hihara and Latanision (Hihara and Latanision, 1994, pp. 251-252) noted in their study about corrosion of graphite-aluminium metal matrix composites (MMC) that proton reduction on graphite will polarise aluminium to noble potentials, explaining the negligible galvanic corrosion rates in de-aerated solutions for MMC. Their results are not directly comparable to ours as the MMC materials differ in structure and purpose of use from graphite-aluminium absorber surfaces. Although our results for samples A-E do not generally match to those for MMC (Hihara and Latanision, 1994) with regard to aeration, it is possible that similar polarising phenomena occurs on the absorber surfaces as well under similar conditions, and may corrode graphite-aluminium absorbers during long-term natural exposure.

As a reference we exposed three absorber samples to non-aerated total-immersion at the room temperature, one at each pH. After 30 days the sample exposed to pH=5.5 was hydrated approximately to the level of PC ≈ 0.5-0.6. Samples exposed to pH = 3.5 and 4.5 did not show any degradation after 70 days by visual inspection.

5. Conclusions

Tests reported in this paper have provided with a general picture on the degradation effect of acid (pH = 3.5 or 4.5) and neutral (pH=5.5) rain on the rough graphite-aluminium solar absorber surfaces at 60, 80 and 99°C. In order to provide more accurate temperature- and time-dependent results the total-immersion test method used needs to be further developed to include controlled movement of solution or sample. Similar to standard tests (draft proposal ISO/CD 12592,2) the main degradation mechanism has been found to be hydration of aluminium oxide (especially at pH = 5.5). It is possible that pH = 3.5 is too acidic for aluminium hydroxides to be formed, thus preventing further corrosion.

For aluminium/aluminium oxide containing samples FTIR-spectroscopy can be used for determining stages of hydration. Thermogravimetry (TG) was useful for determining mass changes indicating water outgassing in highly degraded samples, but smaller degradation rates were not detectable with the TG equipment used.

In our tests we have observed similar degradation for another type commercial aluminium substrate based absorber surface as well. All these results indicate that unglazed solar absorber surfaces based on aluminium substrate need to be well protected against rain diffusion onto the substrate in order to prevent degradation caused by hydration of aluminium oxide.

Acknowledgements

References

Brunold, S., Frei, U., Carlsson, B., Möller K., Köhl, M., 2000a. Accelerated life testing of solar absorber coatings: Testing procedure and results. Sol. Energy 68, 313 – 323.

Brunold, S., Frei, U., Carlsson, B., Möller, K., Köhl, M., 2000b. Round robin on accelerated life testing of solar absorber surface durability. Sol. Energy Mater. Sol. Cells 61, 239 – 253.

Carlsson, B., Frei, U., Köhl M., Möller, K., 1994. Accelerated Life Testing of Solar Energy Materials - Case study of some selective materials for DHW-systems. IEA SHCP Task X.

Carlsson, B., Möller, K., Frei, U., Brunold, S., Köhl, M., 2000a. Comparison between predicted and actually observed in-service degradation of a nickel pigmented anodized aluminium absorber coating for solar DHW systems. Sol. Energy Mater. Sol. Cells 61, 223 – 238.

Carlsson, B., Möller, K., Köhl, M., Frei U., Brunold, S., 2000b. Qualification test procedure for solar absorber surface durability. Sol. Energy Mater. Sol. Cells 61, 255 – 275.

Duffie, J.A., Beckman, W.A., 1991. Solar engineering of thermal processes, second ed. Wiley Interscience, New York.

Hihara, L.H., 1997. Corrosion of aluminium-matrix composites. Corros. Rev. 15, 361-386.

Hihara, L.H., Latanision, R.M., 1994. Corrosion of metal matrix composites. Int. Mater. Rev. 39, 245-264.

Hollands, K.G.T., Karagiozis, A., Shipley, D., 1990. Histograms of Temperature and Humidity of Solar Collector Plate: Phase II and III. IEA SHCP Task X.

Howells, G., 1990. Acid rain and acid waters. Ellis Horwood Limited, Chichester, p. 14.

Konttinen, P., Kilpi, R. Lund, P.D., 2003a. Microstructural analysis of selective $C/Al_2O_3/Al$ solar absorber surfaces. Thin Solid Films 425, 24-30.

Konttinen, P., Lund, P.D., 2003. Thermal stability and moisture resistance of $C/Al_2O_3/Al$ solar absorber surfaces. Sol. Energy Mater. Sol. Cells, accepted for publication.

Konttinen, P., Lund, P.D., Kilpi, R.J, 2003b. Mechanically manufactured selective solar absorber surfaces. Sol. Energy Mater. Sol. Cells 79, 273-283.

Lampert, C.M. (ed.), 1989. Failure and Degradation Modes in Selected Solar Materials: A Review. IEA SHCP Task X.

Magaino, S., 1997. Corrosion rate of copper rotating-disk-electrode in simulated acid rain. Electrochim. Acta 42, 377-382.

Magaino, S., 1999. Zinc corrosion in simulated acid rain. Electrochim. Acta 44, 4307-4312.

Möller, K., SP, Sweden, E-mail dated 21 December 2000.

Shreir, L.L., Jarman, R.A., Burstein, G.T., 1994. Corrosion. Butterworth Heinemann, Oxford, pp. 19:18-19:20.

Takahashi, H., Yamagami, M., Furuichi, R., Nagayama, M., 1987. FTIR Analysis of Hydroxide Films on Aluminum. J. Surface Sci. Soc. Japan 8, 279-281 (in Japanese).

Tanemura, S., Yoshimura, K., Taga, K., Odaira, R., Ishida, M., Tsuboi, S., Yoshikawa, M., 1990. Accelerated aging testing of Ni pigmented anodized Al under heat and/or high humidity loads and degradation mechanism. In: Horigome, T., Kimura, K., Takakura, T., Nishino, T., Fujii, I., (Eds.), Proceedings of the 1989 Congress of the International Solar Energy Society, 4-8 September 1989, Kobe City, Japan. Pergamon Press.

Tarvainen, V., Finnish Meteorological Institute, E-mail dated 3 March 2003 (based on Rogers, R.R., Yau, M.K., 1989. A short course in cloud physics, Pergamon Press, p. 191)